



**HAL**  
open science

## Smoke layer / water spray interaction – Thermal and radiative characterization

Elizabeth Blanchard, Gilles Parent, Silvio Renard, Philippe Fromy, Pascal Boulet, Didier Borgiallo

► **To cite this version:**

Elizabeth Blanchard, Gilles Parent, Silvio Renard, Philippe Fromy, Pascal Boulet, et al.. Smoke layer / water spray interaction – Thermal and radiative characterization. Interflam 2016 - 14th International Conference and Exhibition on Fire Science and Engineering, Interscience Communications, Jul 2016, Windsor, United Kingdom. hal-01578160

**HAL Id: hal-01578160**

**<https://hal.univ-lorraine.fr/hal-01578160>**

Submitted on 29 May 2023

**HAL** is a multi-disciplinary open access archive for the deposit and dissemination of scientific research documents, whether they are published or not. The documents may come from teaching and research institutions in France or abroad, or from public or private research centers.

L'archive ouverte pluridisciplinaire **HAL**, est destinée au dépôt et à la diffusion de documents scientifiques de niveau recherche, publiés ou non, émanant des établissements d'enseignement et de recherche français ou étrangers, des laboratoires publics ou privés.

# SMOKE LAYER/WATER SPRAY INTERACTION – THERMAL AND RADIATIVE CHARACTERIZATION

Elizabeth Blanchard<sup>(1)</sup>, Gilles Parent<sup>(2,3)</sup>, Silvio Renard<sup>(1)</sup>, Philippe Fromy<sup>(1)</sup>, Pascal Boulet<sup>(2,3)</sup>,  
D. Borgiallo<sup>(4)</sup>

- (1) CSTB (Centre Scientifique et Technique du Bâtiment) - Université Paris Est, 84 avenue Jean Jaurès Champs sur Marne, 77447 Marne-La-Vallée cedex 2, France
- (2) Université de Lorraine, LEMTA, CNRS UMR 7563, TSA 60604 Vandœuvre-lès-Nancy, F-54518, France
- (3) CNRS
- (4) PROFOG, Parc Activité Moulin de Massy, 39 rue du Saule Trapu, 91 300 Massy, France

## ABSTRACT

The present study deals with smoke layer / water spray interaction. It is based on a 16-test campaign conducted at real scale. The test set-up consists in a room connected to a corridor. The smoke is generated with an heptane pool in the room, the spray is operating in the corridor. There is no interaction between fire activity and spray operation. Instrumentation allows to measure heat release rate of the pool fire, gas temperature along the corridor and radiative attenuation along vertical axis. The present study deals with the impact of two different sprays on the smoke layer. The instrumentation is used to characterize the corridor environment.

**KEYWORDS:** Smoke/spray interaction, real scale experimentation

## INTRODUCTION

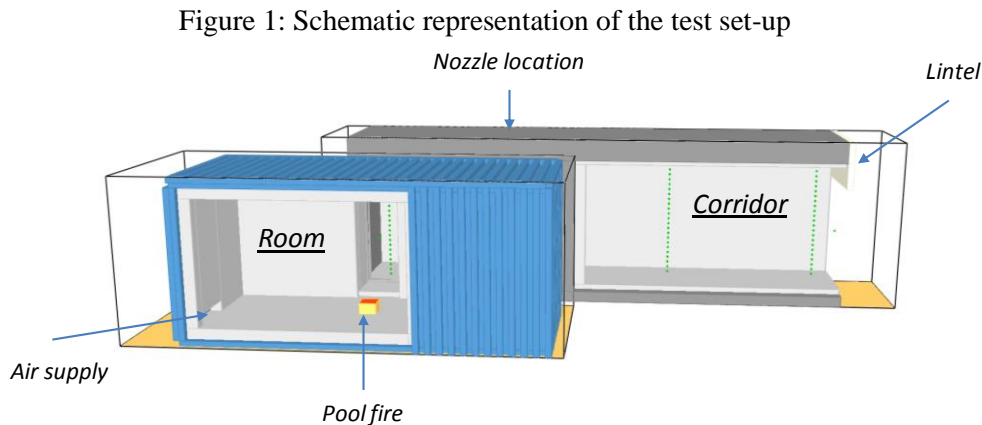
When water is sprayed in a fire environment, droplets impact the fire activity and interact with the smoke layer, and the building walls. Many well-known phenomena are involved, among them gas cooling, radiative attenuation, momentum transfer. However, it is still difficult to quantify their respective role. Indeed, their contribution depends on both fire and water spray characteristics. For instance, sprinkler systems involve large droplets with high inertia leading to surface cooling, whereas water mist is rather expected to promote a strong evaporation leading to gas cooling, in addition to enhanced thermal radiation attenuation, while the corresponding droplets are less able to reach surfaces due to lower droplet inertia.

Our research is about the interaction between smoke layer and water spray. Two different technologies are tested, a water mist system and a sprinkler system. The test set-up consists in a room connected to a corridor. The smoke is generated with an heptane pool in the room, the spray is operating in the corridor. In the present study, we aim at characterizing the interaction between smoke layer and water spray by considering two types of data, gas temperature and radiation attenuation. The idea is to characterize this interaction through these two quantities where thermal and optical aspects are likely decoupled (cf. Ref. <sup>1,2</sup>). Indeed, the two tested systems are selected since they induce the same impact in the corridor on the thermal aspect: well-mixed steady-state conditions along the corridor with strong smoke cooling and mixing with fresh air. In addition, opacimetry give indication about the local physical properties since radiative properties are associated to the presence of mixed soot and droplets.

## TEST DESCRIPTION

### Test set-up

The real-scale test set-up is described with details in Ref<sup>1</sup>. A schematic representation is given on Figure 1. It is made up of a room which adjoins a corridor. The room surface area is about 12 m<sup>2</sup> and 2.15 m high. The corridor is 9 m long, 1.4 m wide and 2.4 m high. An opening is made in the room, close to the floor, in order to ensure air supply to the fire during the whole test duration. A lintel is built at the corridor extremity to promote a thick and homogeneous smoke layer in the corridor.



The fire load is burning in the room, at its centre. It is an heptane pool fire with a surface area of 0.10 m<sup>2</sup>.

The water spray operates in the corridor at 3.5 m from the corridor extremity close to the room (cf. Figure 2). The nozzle is close to the ceiling. Its position and the fire load position as well allow to limit interaction between fire activity and spray operation. In that way, water spray interacts only with the smoke layer produced by the fire and flowing below the ceiling along the corridor.

Two water sprays are studied, one high-pressure water mist system and one sprinkler system. The water mist system is operating at 85 bars with a corresponding delivered flow rate of about 25 L/min. The nozzle is spraying droplets through its six lateral orifices. The water droplet mean diameter measured with a Malvern diffractometer is comprised between 110 and 160 µm, between 40 cm and 1 m from the nozzle location, along the central vertical axis. The sprinkler system is operating at 1.3 bars with a corresponding delivered flow rate of 91 L/min. Water droplet mean diameter is measured with the diffractometer too. It is found to be unexpectedly low, between 170 and 230 µm, between 40 cm and 1 m from the nozzle location, along the central vertical axis. Note that the central vertical axis corresponds to the intersection of the six sprays delivered by the water mist system. For the sprinkler system, it corresponds to a zone where no droplet is sprayed directly.

### Instrumentation

Three quantities are measured, the heptane pool mass, gas temperature and also opacity.

Heat release rate (HRR) is deduced from the pool mass loss rate, following the simple relationship

$$\text{HRR} = \eta \Delta m_p \Delta H_c \quad [1]$$

where  $\eta$  is the combustion yield,  $\Delta m_p$  (in kg/s) is the measured pool mass loss rate and  $\Delta H_c$  (in kJ/kg) is the heat of combustion for heptane equal to 44 600 kJ/kg.

Gas temperature is measured along one 14-thermocouple tree at the junction between the room and the corridor. Gas temperature is measured along six other 18-thermocouple trees in the corridor, at regular

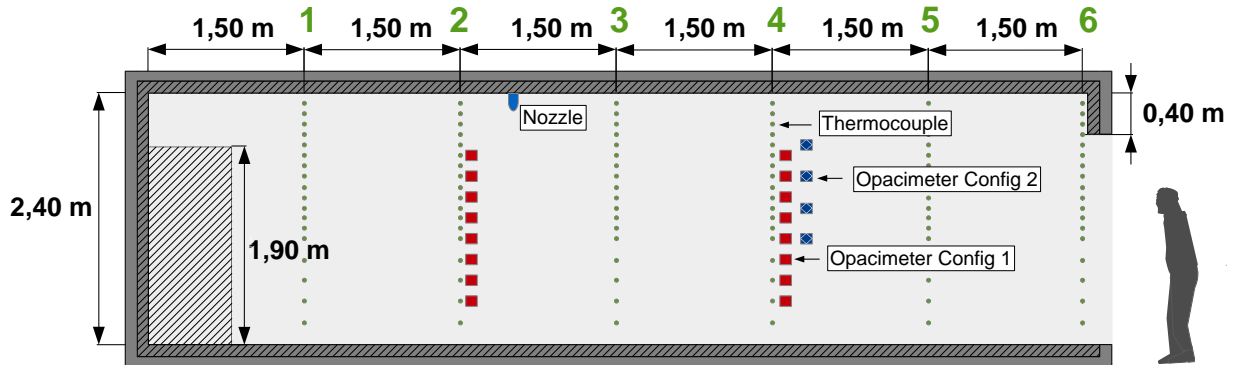
distance, every 1.5 m (see Figure 2). Thermocouples are located along each tree between 20 cm from the floor and 10 cm below the ceiling. The distance between thermocouples is narrower from mid-height up to the ceiling in order to better characterize the presence of smoke, before spray activation. There are 122 thermocouples in total. Figure 2 indicates the position of the thermocouple trees. As shown, trees are as well upstream the spray and downstream the spray.

Opacity is measured along trees of opacimeters. A laser source emits a light at a given wavelength which is transmitted to a photo-diode after having travelled through gas containing smoke with possibly droplets in suspension. The type of used opacimeter is deeply presented in Ref<sup>2</sup>. Light transmissivity T is deduced from the ratio between the intensity measured during the test I and the intensity before fire ignition  $I_0$  as follows

$$T = I / I_0 \quad [2]$$

Two arrangements of opacimeters are used in the test campaign, either two 8-opacimeter trees at a single wavelength (referred as Config 1 on Figure 2), or one 16-opacimeter tree at four different wavelengths (referred as Config 2 on Figure 2). In Config 1, one tree is located upstream the spray at section 2 and one downstream at section 4. On each tree, there are 8 opacimeters, between 40 cm and 1.8 m high from the floor, with a spacing of 20 cm. The optical path is 30 cm between emission and reception. The light is emitted at a given wavelength 642 nm. In Config 2, there is only one tree in the corridor, at a position corresponding to section 4. Sixteen opacimeters are along the tree, at four different heights, from 1 m up to 1.9 m high, with a spacing of 30 cm. At each height, four opacimeters measure light transmissivity at four different wavelengths in the visible range, 405 nm, 520 nm, 642 nm and 785 nm. The optical path is the same as in Config 1, 30 cm between emission and reception.

Figure 2: Position of the measurement sections in the corridor. Dots represent thermocouples, squares opacimeters. Nozzle location is represented by a blue shape. Numbers refer to the number of measurement section (longitudinal cross-section view)



### Test campaign and test protocol

Here are presented the results from two test series. The first series is composed of ten tests, five repeatability tests per technology, and the opacimeter arrangement is in Config 1. The first series is deeply presented in Ref<sup>1</sup>. The second series is composed of six tests, three tests per technology and the opacimeter arrangement is in Config 2.

The test protocol is similar in both test series. The test starts when fire is ignited. After seven minutes, spray is activated manually. Spray operates during five minutes, until twelve minutes. The fire ends when heptane is totally consumed, after approximately 30 minutes. Only the first fifteen minutes are studied. This time period corresponds to the fire growth phase followed by the steady state period.

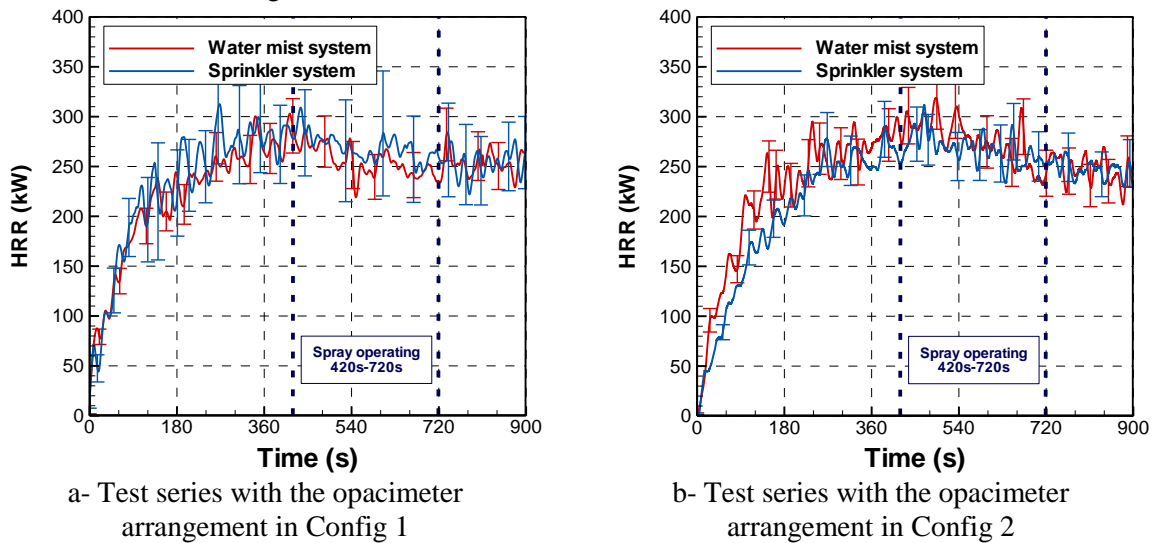
### MEASUREMENTS

#### Heat release rate

During the first fifteen minutes, HRR evolution has two stages, a fire growth phase during around 300 s and a steady stage after. The steady HRR value is comprised between 250 and 300 kW. Figure 3 plots temporal evolution of HRR measured in both test series, corresponding to the two opacimeter arrangements Config 1 and Config 2.

As mentioned previously, there is no direct interaction between fire activity and water spray, water interacts only with the smoke layer. The goal is to compare the two technologies in the same condition without impacting fire activity and consecutive smoke production. In consequence, HRR is similar whatever the technology, water mist system or sprinkler system. Moreover, HRR is hardly affected by spray operation between 420 and 720 s, HRR remains at its steady value. Between the two test series, the test protocol is identical. Thus, HRR deduced from pool weight loss monitoring is the same.

Figure 3: HRR versus time measured in both test series



### Before spray activation

Before spray activation, temperature and transmissivity follow the same temporal evolution as HRR. Temperature increases and transmissivity decreases with HRR. Only a difference is observed for gas temperature after around 300 s. Indeed, whereas HRR is almost at its steady value, temperature continues to increase. It is due to heat exchanges with walls: the temperature difference between walls and gas decreases with time as wall are being hotter and hotter.

As Figures 4 and 5 illustrate, there is a stratification in the corridor with a smoke layer in the upper part and some fresh air in the lower part. As a consequence, temperature increases with height while transmissivity decreases due to the presence of hot and dark smoke. This stratification is more obvious on Figure 6. To draw this figure, a mesh is created with nodes corresponding to thermocouple positions. Gas temperature measured locally with thermocouples is set to nodes. A visualization tool interpolates linearly temperatures between nodes and colours the values also get. On Figure 6 too, are plotted the transmissivity vertical profiles measured at sections 2 and 4 in Config 1. This figure demonstrates more obviously temperature and transmissivity measurements are coupled before spray activation. In particular, at the corridor mid-height, at 1.2 high, gas temperature is slightly hotter than ambient temperature and transmissivity is slightly lower than 1 traducing the presence of diluted smoke. Moreover, Figure 6 illustrates heat exchanges between walls and smoke layer. Smoke is cooled as it is flowing along the corridor, its maximum temperature decreases along the longitudinal direction, from 160 °C at section 1 to 125 °C at section 6 at 2.3 m high.

Figure 4: Temperature and transmissivity versus time measured at different elevations at section 4, for water mist system, with the opacimeter arrangement in Config 1

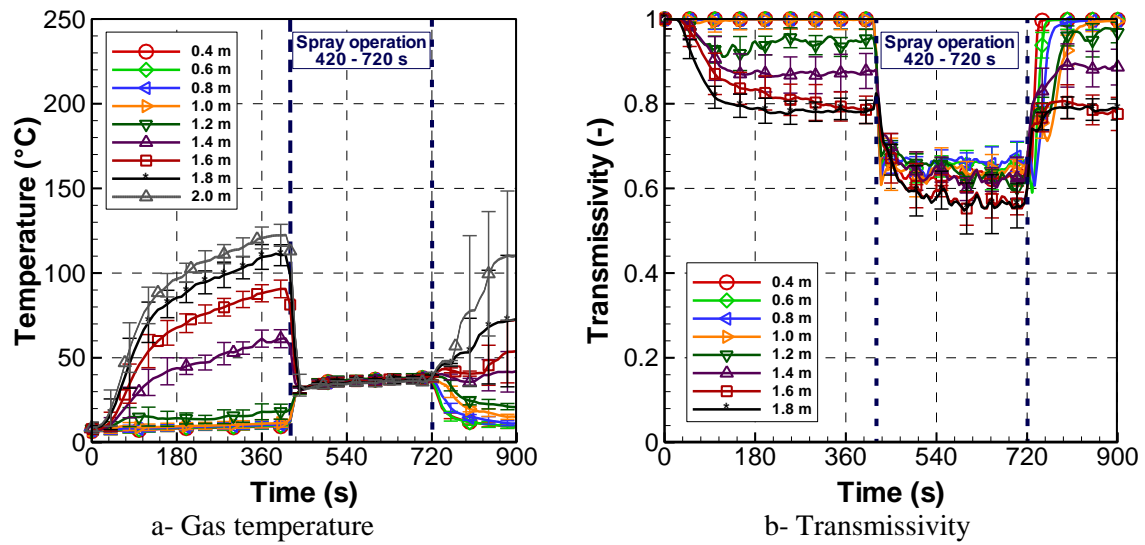


Figure 5: Temperature and transmittance versus time measured at different elevations at section 4, for sprinkler system, with the opacimeter arrangement in Config 1

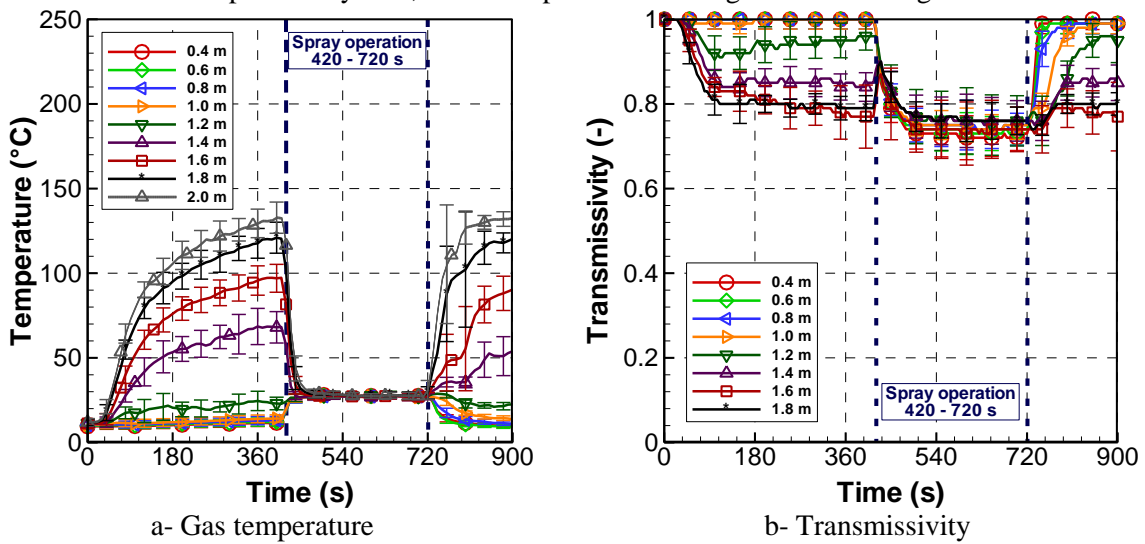
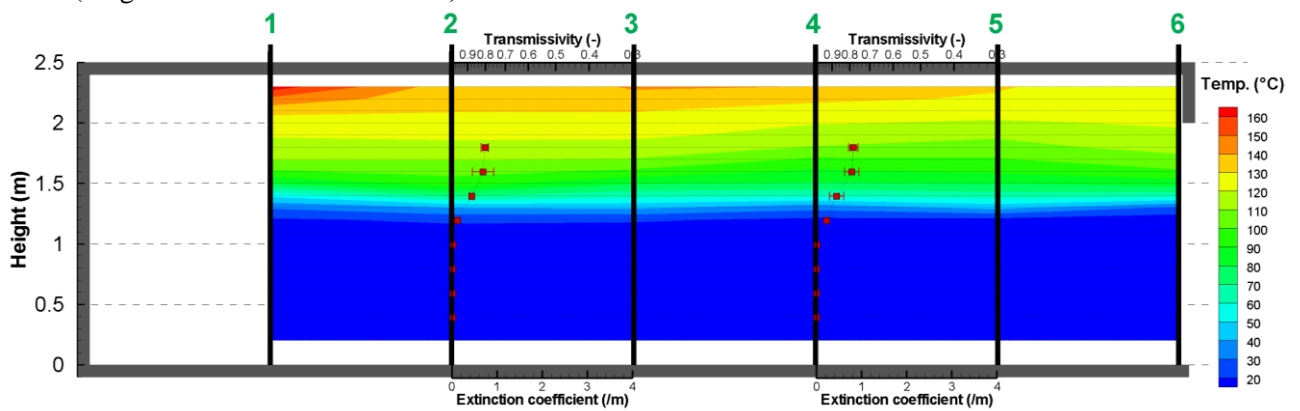


Figure 6: Temperature contour in the corridor at 360 s with transmissivity profiles plotted at sections 2 and 4 (longitudinal cross-section view)



After spray activation, during spray operation

When spray is activated, water mist system and sprinkler system have a similar impact on temperatures in the whole corridor. As Figures 4-a and 5-a shown, spray induces well-mixed steady-state conditions along the corridor with strong smoke cooling and mixing with fresh air. Gas temperature, with a maximum value around 135 °C before spray activation between sections 2 and 6, drops and becomes homogenous with height, with a mean temperature around 30 °C/35 °C for both systems. Figures 7 and 8 present in the same manner as Figure 6 gas temperatures measured in the corridor during spray operation at 600 s. On these two figures, the temperature homogenization is more obvious between sections 3 and 5. Figures 7 and 8 show mass flow through the corridor extremities: smoke is still flowing from the room (fire activity is not affected by spray) and fresher air is still flowing from the outside. Smoke is traduced on Figures 7 and 8 by higher temperatures close to the ceiling measured at sections 1 and 2 i.e. upstream the spray and also almost below the spray. Fresher air appears on Figures 7 and 8, downstream the spray, along a distance between 1.5 and 2 m from the corridor extremity.

Figure 7: Temperature contour in the corridor at 600 s with transmissivity profiles plotted at sections 2 and 4 (longitudinal cross-section view), for water mist system

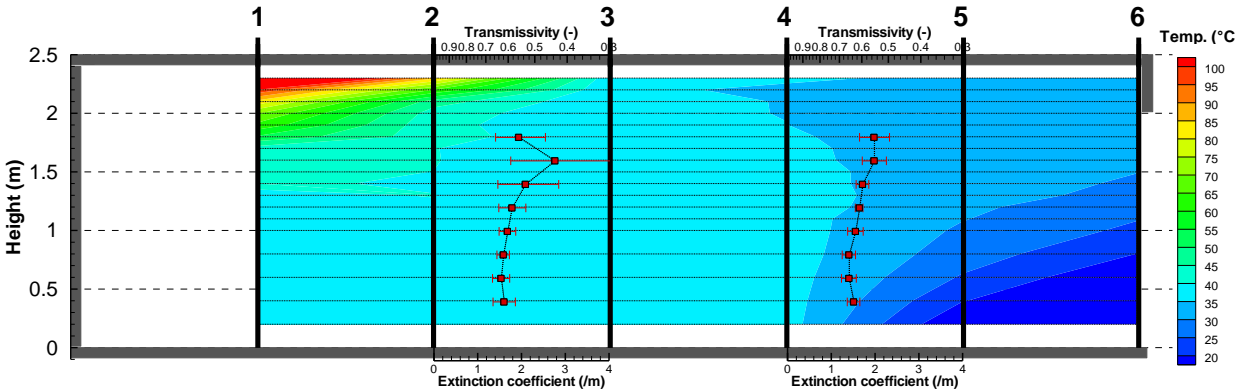
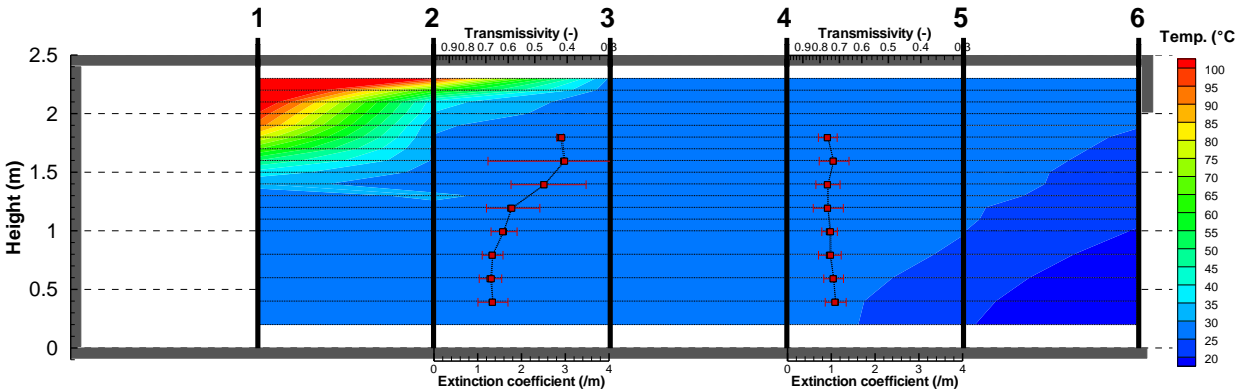


Figure 8: Temperature contour in the corridor at 600 s with transmissivity profiles plotted at sections 2 and 4 (longitudinal cross-section view), for sprinkler system



Figures 7 and 8, associated to Figures 4-b and 5-b, show the impact of spray operation on transmissivity. It appears more contrasted, temporarily and spatially in comparison to temperature. Temporarily, at section 4, spray impact is progressive on transmissivity for both technologies while temperature becomes homogenous almost instantaneously at this position. Indeed, spray activation induces a progressive decrease in transmissivity during the two first minutes of spray operation. After this decrease, transmissivity remains almost steady during the whole spray operation period. Spatially, the steady value of transmissivity depends on the vertical sensor position, the measurement section and the technology. With water mist system, the measured transmissivity decreases with height and it is similar between sections 2 and 4: it is comprised between 0.4 and 0.65 at section 2 and between 0.55 and 0.65 at section 4. With sprinkler system, the measured transmissivity is different between

sections 2 and 4. At section 2, transmissivity decreases with height. It is equal to 0.7 below 0.8 m high and between 0.4 and 0.46 above 1.2 m. At section 4, it is almost constant, around 0.75.

## ESTIMATION OF THE LOCAL COMPOSITION

### Before spray activation

Laser beam attenuation is attributed to absorption and scattering phenomena. The Beer-Lambert's law relates measured transmissivity  $T$  to the extinction coefficient  $\beta$ , the sum of absorption and scattering coefficients, as follows

$$T = \exp(-\beta L) \quad [3]$$

where  $L$  is the path length equal to 30 cm. In this law, multiple scattering phenomenon is neglected.

As demonstrated in Ref<sup>6</sup>, the extinction coefficient is linearly related to the soot mass concentration  $C_{m,s}$  (in  $\text{kg}/\text{m}^3$ ) with mass specific extinction coefficient  $K_m$  (in  $\text{m}^2/\text{kg}$ ) as follows

$$\beta = K_m C_{m,s} \quad [4]$$

Mulholland in Ref<sup>3</sup> summarizes experimental value from seven test campaigns involving 29 fuels. The listed values corresponding to heptane are 7.8 and 10.3  $\text{m}^2/\text{g}$  at 632.8 nm. By extending these values to the transmissivity at 642 nm, a range for the local soot mass fraction is estimated. The minimum value corresponds to a mass specific extinction coefficient equal to 10.3  $\text{m}^2/\text{g}$ , the maximum value to a mass specific extinction coefficient equal to 7.8  $\text{m}^2/\text{g}$ . Figure 9 summarizes the values at both sections 2 and 4, with vertical profiles, at 360 s. This figure shows the soot mass concentration has a similar profile as temperature, it is different to zero from 1 m from the floor up to the corridor ceiling and it increases with height. At the highest opacimeter, at 1.8 m high, the maximum estimated value of soot mass concentration is around 0.07-0.09  $\text{g}/\text{m}^3$  at section 2 and around 0.08-0.11 at section 4.

Figure 9: Soot mass concentration versus corridor height, at sections 2 and 4 at 360 s

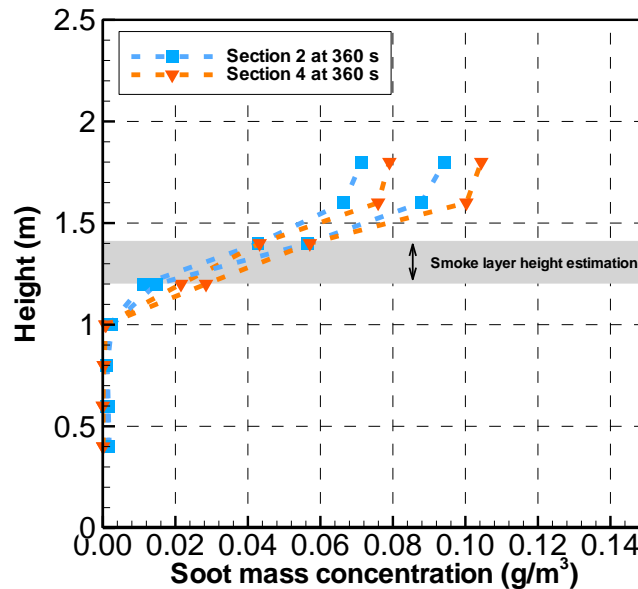


Figure 10 presents the vertical profiles of transmissivity measured in the test campaign with Config 1 and in the test campaign with Config 2. As it is shown, there is a good agreement between the dot curve and the dots corresponding to a wavelength equal to 642 nm, in Config 1 and Config 2 respectively. It also confirms both test series are similar and can be studied complementary.



Figure 10: Transmissivity versus height with Config 1 and 2, at section 4 at 360 s

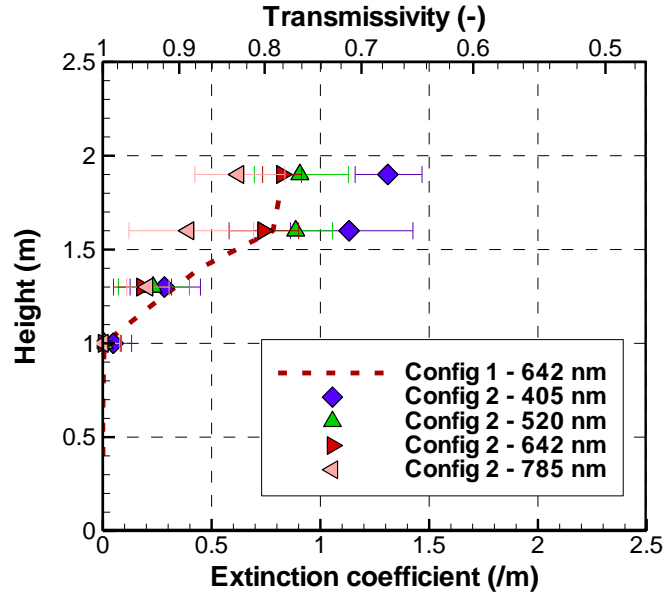


Figure 10 shows also that there is difference in transmissivity value between the four wavelengths. Indeed there is a dependency of the extinction coefficient to the wavelength. The soot particles being considerably smaller in diameter than the wavelength in the visible range, the size parameter  $\pi D/\lambda$  is much less than 1. For very small particles the Rayleigh theory applies. It implies that the scattering cross section is proportional to  $(\pi D/\lambda)^4$  and the absorption coefficient to  $(\pi D/\lambda)$  (see Ref<sup>4</sup>).

The soot spectral absorption  $\kappa$  is often related to the soot volume fraction  $f_v$  and the wavelength as follows (see Ref<sup>4</sup>)

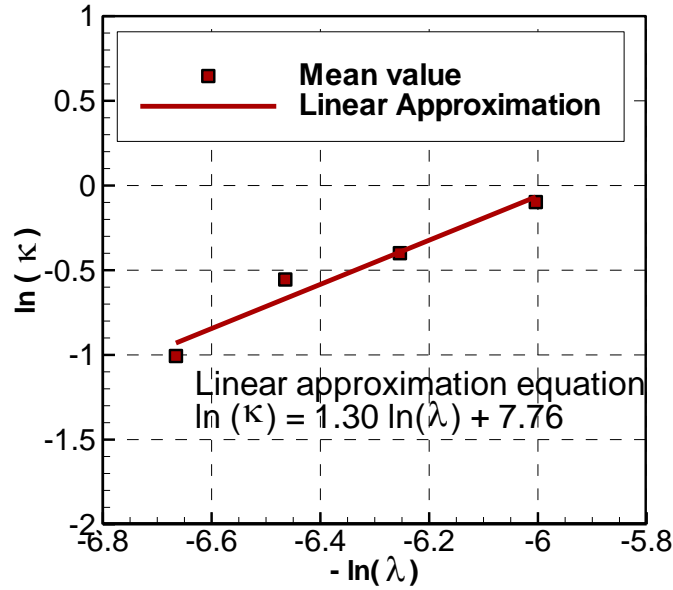
$$\kappa = (f_v C) / \lambda^\alpha \quad [5]$$

where  $k$  and  $C$  are constants. The constant  $k$  integrates soot complex index and soot density. The constant  $\alpha$  in Equation 5 can be estimated by applying a linear regression method by supposing a negligible wavelength dependence of the scattering coefficient  $\sigma$

$$\ln(\beta - \sigma) = \ln(f_v C) - \alpha \ln(\lambda) \quad [6]$$

Following the Mie theory, soot scattering is much lower than absorption. However, previous studies point out the ratio of the scattering to extinction coefficient is not negligible in the visible range. The ratio is comprised between 0.18 and 0.3 in Ref<sup>5</sup> at 632 nm regarding the fire load type. In Ref<sup>6</sup>, the ratio is comprised between 0.195 and 0.311 and depends on both the fire load type and the wavelength. By supposing that scattering coefficient  $\sigma$  is equal to 30 % of the extinction coefficient and that this proportion does not vary with the wavelength, we estimate the constant  $\alpha$  from measurements at 1.6 and 1.9 m high from the floor. Its mean value is equal to 1.3 during the time period [300 s ; 420 s]. This value is in the range of the scientific literature (see Ref<sup>4</sup>). The corresponding linear approximation is plotted on Figure 11 with associated measurements.

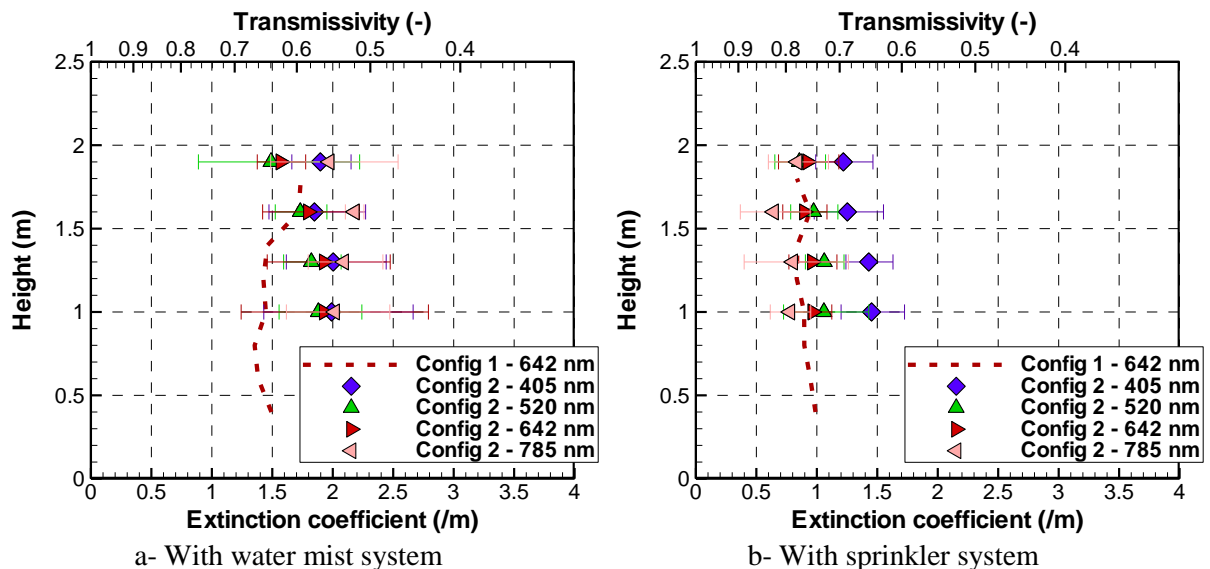
Figure 11:  $\ln(\kappa)$  versus  $\ln(\lambda)$



**After spray activation, during spray operation**

As said previously, water mist and sprinkler have similar impact on gas temperature along the corridor whereas their impacts on transmissivity differ. Moreover, whereas gas temperature becomes almost homogeneous along the corridor with a strong smoke cooling, transmissivity measurements lead to a more contrasted impact differing temporarily and spatially. Figure 12 plots the vertical profile of mean transmissivity during spray operation [420 s; 720 s]. The dot curve represents the measured transmissivity in the test series with Config 1, the dots the measurements with Config 2. As it is shown, there is a good agreement between the dot curve and the dots corresponding to a wavelength equal to 642 nm, in Config 1 and Config 2 respectively. The curve is in the overlap of the error bars which traduces a good repeatability of the test protocol.

Figure 12: Transmissivity versus height with Config 1 and 2, at section 4 during spray operation



Like before spray activation, there is a difference in transmissivity value between the four wavelengths. Indeed there is a dependency of the extinction coefficient to the wavelength. However, this dependency differs between water mist and sprinkler system. With sprinkler system, higher the wavelength is, higher the transmissivity is measured and smaller the extinction coefficient is. Moreover, the logarithm of the transmissivity varies linearly with the logarithm of the wavelength. The constant  $\alpha$  in Equation 5

estimated as previously is around 0.77. With water mist system, it appears trickier to identify the dependency of transmissivity with wavelength. The maximum value is at 520 nm and the minimum value at 785 nm. The difference of dependency is interpreted as the loss transmissivity with water mist is more due to the presence of droplets mixed with soot while the loss transmissivity with sprinkler is more attributed to the presence of soot.

## CONCLUSION

The present study is about the interaction between smoke layer and water spray. It is based on two series of large scale fire tests. Two water sprays are studied, a water mist system and a sprinkler system. Our goal is to examine the interaction considering two types of data, gas temperature and radiation attenuation. For that, several trees of thermocouples and opacimeters are installed in the test set-up. Results show that both quantities traduce a different impact of water spray on smoke layer. Temperatures indicate well-mixed steady-state conditions along the corridor with strong smoke cooling and mixing with fresh air. Opacimetry measurements show a more contrasted impact with remaining variation of transmissivity within the corridor. In addition, opacimetry give indication about the local physical properties since radiative properties are associated to the presence of mixed soot and droplets. Also, a soot concentration is evaluated before spray activation. Moreover, during spray operation, transmissivity measurements seem to indicate that loss of visibility is more due to the presence of soot with sprinkler systems while it seems to be due to mixed droplets in suspension and soot with water mist system.

## REFERENCES

<sup>1</sup> E. Blanchard, R. Morlon, G. Parent, P. Fromy, P. Boulet and D. Borgiallo, “Experimental study of the interaction between water sprays and smoke layer”, *Fire Technology*, Vol. in press (2016)

<sup>2</sup> G. Parent, R. Morlon, P. Fromy, E. Blanchard and P. Boulet, “Opacity measurement in a fire environment using a network of optical fibres”, *Fire Safety J.*, Vol. in press (2016)

<sup>3</sup>G. W. Mulholland and C. Coarkin “Specific extinction coefficient of flame generated smoke”, *Fire and Material*, Vol. 24, pp 227-230 (2000)

<sup>4</sup> R. Siegel and J. R. Howell “Thermal radiation heat transfer”, 2<sup>nd</sup> edition, series in thermal and fluids engineering

<sup>5</sup> F. X. Ouf “Caractérisation des aérosols émis lors d’un incendie”, PhD thesis, Université de Rouen, 2006

<sup>6</sup>J. Zhu, M. Y. Choi, G. W. Mulholland and L. A. Gritzo “Soot scattering measurements in the visible and near-infrared spectrum”, *Combustion institute*, Vol. 28, pp 439-446 (2000)